Absolute total cross sections for electron-mercury scattering

K. Jost and B. Ohnemus
Physikalisches Institut, Westfälische Wilhelms Universität, Münster, Germany
(Received 25 April 1978)

The total cross section for e^--Hg scattering has been measured in the energy range between 0.1 and 500 eV. Absolute data taken at a few energies by means of a static target were used to normalize the relative cross sections, which were measured in the whole energy range by scattering from an atomic beam. This technique was used to help meet the high-angular-resolution requirements. The cross sections obtained are considerably larger than those obtained in most of the other measurements performed around 1930. Satisfactory agreement is found, however, with semiempirical cross sections (mainly based on recent measurements) and with a recent theoretical calculation. The most pronounced structure is a cross section maximum at 0.4 eV, which probably can be ascribed to a $(6s\,^2 6p_{1/2})^2P_{1/2}$ shape resonance.

INTRODUCTION

Among the heavy atoms, mercury is probably the most favored target for low-energy-electron scattering experiments, because it is easy to evaporate and to condense. A large number of experimental differential cross sections[1] of electrons scattered from mercury is available as well as detailed spin-polarization values.[2]

Nevertheless, there are surprisingly few measurements of the total cross section,[3-6] and moreover these are not very recent. These old data are now considered to be rather unreliable.[7] More recent measurements of momentum transfer cross sections[8,9] have been made, but these are not identical with the total cross section, unless special requirements, such as isotropic scattering, are fulfilled.[7,10,11(a)] Some further recent measurements concentrate on the location of the energies and studies of the shape of sharp structures in the cross section, without being designed to determine the cross section itself.[12-17] These, and the momentum transfer data will be called "indirect measurements" in the following.

In addition to their use for estimates of scattering intensity, reliable measurements of the total cross section of mercury are of some theoretical interest, because they are important for a phase-shift analysis[18,19] of experimental data. Furthermore, theoretical approximations can be checked: Depending on the approximation being used,[20,21] the total cross sections obtained either decrease monotonically with increasing electron energy, or maxima—and even shape resonances—can occur at about 1 eV or below. Most of the older direct measurements[3-6] are consistent with the total cross section decreasing monotonically, which is therefore also stated in modern textbooks.[11(b)] A maximum is indicated, however, by the indirect measurements[8-10,14,15] as well as by the phase-shift analysis.[18,19]

The present experiment is designed to measure the total cross section by the attenuation method down to sufficiently low energies to help clarify the above problems. First the relative shape of the cross section versus energy was determined in the energy range between 0.1 and 500 eV, employing an atomic beam target. Then absolute data were taken at selected energies around 20 eV using a static vapor cell with known geometry. This way it was possible to get an absolute cross-section curve over the whole energy range without renouncing the advantages of an atomic beam target which are especially important at the boundaries of the energy interval under investigation. The use of an atomic beam facilitates both the achievement of a high angular resolution and the avoidance of target vapor reaching the cathode, where energy shifts by gas cooling or by modification of the work function could occur. At low energies, even small energy shifts would be disturbing. At higher energies, where forward scattering is more pronounced, a high angular resolution is necessary in order to distinguish between scattered and unscattered electrons.

Although magnetic fields facilitate the handling of narrow beams of slow electrons, they have been avoided throughout in order to get a simple scattering geometry, which facilitates analysis of the data. The electron beam was monochromatized and focused entirely by electrostatic means and the scattering itself occurred in a field-free region.

GENERAL LAYOUT OF THE APPARATUS

Three different setups have been used for the cross-section measurements, each consisting of an electron gun, an electron optical system for beam transport, a target cell, and a Faraday cup

as a collector. The relative measurements were performed in two widely overlapping energy ranges using the atomic beam target. At low energies between 0.1 and 70 eV, a monochromator was employed; the complete arrangement is shown in Fig. 1. At higher energies, between 20 and 500 eV, the monochromator was removed. The electron optical system for the latter measurements is shown in Fig. 2, whereas the target arrangement was the same as in Fig. 1. Finally, in order to measure absolute cross sections in the energy range from 15 to 30 eV, the electron optical setup of Fig. 1 was again used. The atomic beam target was replaced, however, by a static target cell (Fig. 3).

These systems were mounted alternately in a vacuum vessel of nonmagnetic stainless steel, which is pumped by a mercury diffusion pump through a refrigerated baffle and a liquid-nitrogen baffle. After mild baking at about 100 °C, a pressure of 10^{-8} Torr was reached. During the measurements, the pressure in the vacuum chamber could rise to some 10^{-7} Torr, depending on the temperature of the mercury oven.

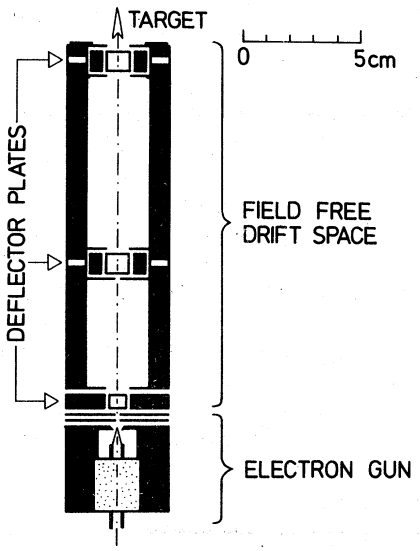

FIG. 2. Electron optical arrangement for higher energies (20–500 eV). This is used in conjunction with the target of Fig. 1.

The Earth's magnetic field was reduced to below 0.5 mOe in the region of the electron beam path by large Helmholtz coils and a magnetic shield surrounding the vacuum chamber. Current leads to heaters (mercury oven, scattering cell) and to the hairpin cathode were either bifilar or coaxial; no influence of the remaining stray fields on the electron beam could be detected when the heaters were switched on and off deliberately or when the polarity of the dc power supply to the cathode was changed. All materials used in the apparatus were carefully checked for being nonmagnetic. In the following sections, more details on the operation of the components will be given.

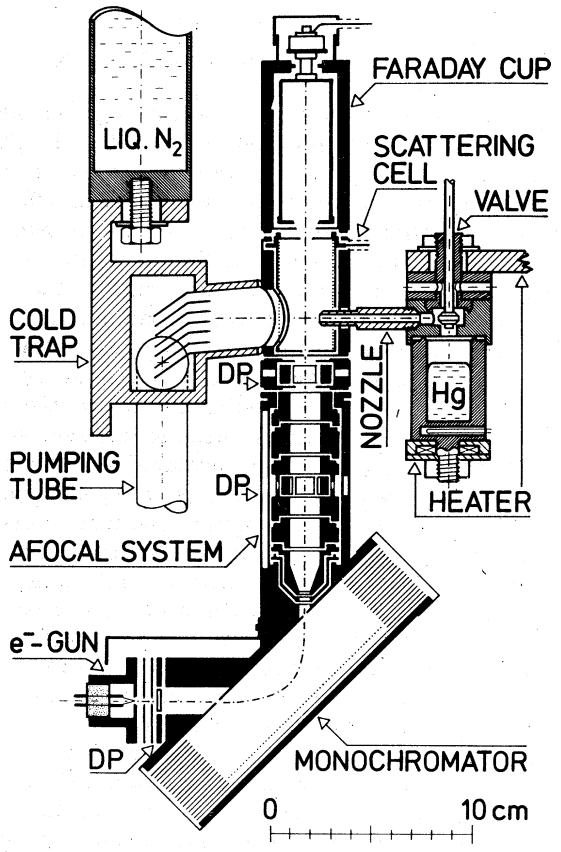

FIG. 1. Electron optical arrangement for low energies (0.1–70 eV) with atomic beam target. Deflector plates are denoted by DP.

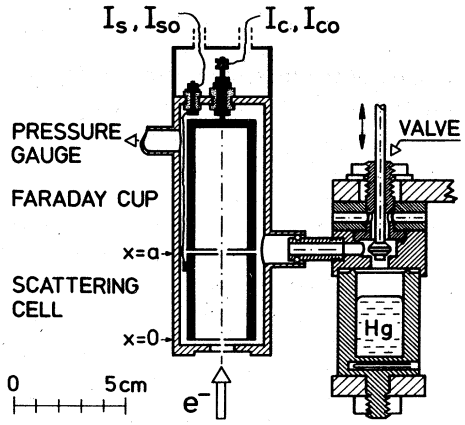

FIG. 3. Target cell for absolute measurements. This arrangement is used together with the electron optics of Fig. 1.

ELECTRON OPTICAL SETUP FOR LOW ENERGIES (0.1-70 eV)

This arrangement is shown in Fig. 1. A constant potential difference of 5 V was maintained between the tip of a tungsten hairpin cathode and the entrance slit of a parallel-plate monochromator.[22] Therefore, the electrons are always energy selected at the same energy. The monochromator is built of molybdenum. Its entrance and exit slits are 0.4 mm wide by 1.5 mm long, separated by 60 mm. A set of correction plates at appropriate potentials ensures a homogeneous field. The repelling electrode is a Mo micromesh (mesh size 0.25×0.25 mm, transparency 85%) through which nonselected electrons may escape. Furthermore, the electron beam entering the device can be checked behind the mesh if no electric field is maintained between the plates.

After passing the monochromator, the electrons are either decelerated or accelerated to the desired energy by a seven-element afocal system.[23,24] The last lens element is grounded in order to avoid field penetration into the scattering cell which is also at ground potential. This also helps to avoid excessive angular spread of the electron beam due to lens action just in front of the 1-mm diam. aperture of the scattering cell. Because of contact potentials and thermal energy, the electron energy was not given exactly by the voltage difference between cathode and ground potential. For the same reason it was not possible to run the afocal system with the voltage ratios given in the literature. Nevertheless, these values were a valuable guide and a sufficiently energy-independent current could be obtained to plot the resonances in the transmitted current versus energy by means of an xy recorder with greatly suppressed zero. The resonances were used for energy calibration.

During the measurements of the cross sections, where larger energy variations were necessary, the voltages of the lens elements and deflector plates of the afocal system were optimized individually for each energy. It was important, however, not to change any of the potentials between the cathode and the exit slit of the monochromator, because otherwise an unintentional energy shift could occur by selecting a different portion of the broad thermal-energy distribution of the electrons.

ELECTRON OPTICAL SETUP FOR HIGHER ENERGIES (20-500 eV)

Essentially, the same hardware as above was used, but without the monochromator. All the lens elements of the former afocal system and the scattering cell were at ground potential. Therefore, in Fig. 2 the individual elements, being at the same potential, are not shown separately. Furthermore, several narrow apertures were inserted into the lens elements of the afocal system. The philosophy behind this procedure is the following: The electrons are accelerated to the desired energy in the comparatively short electron gun (formerly in front of the monochromator). The electrons then enter the former afocal system, which now serves as a long, field-free drift space without any lens action. By directing the electron beam step by step through the small apertures by means of the deflector plates, a well-collimated small-diameter beam results. At higher energies, a beam of small angular divergence is more important than a beam of small energy spread. This is because at higher energies the forward scattering increases, whereas the energy dependence of the total cross section to be measured decreases. Therefore, the thermal-energy spread can be tolerated here, and also the disturbing influence of contact potentials on the energy determination becomes less important.

SCATTERING CELL AND ELECTRON DETECTION

The relative measurements have been performed using the atomic beam target shown in Fig. 1. The atomic beam can be quickly switched on and off by the pneumatically activated valve. About 80% of the controlled heating power is fed to the oven across the valve unit on top of the reservoir in order to keep this part, which also carries the nozzle, hotter than the mercury supply itself. This way, condensation of mercury vapor in the nozzle was avoided. An additional heater at the bottom of the reservoir supplies the rest of the heating power. A Pt sensor close to this second heater shows only small temperature oscillations due to heater switching (<0.5 °C peak to peak) and no detectable temperature drifts. Because of thermal time lags, the temperature of the mercury supply itself is even more stable and an atomic beam of constant intensity (within <1%) could be obtained. The nozzle is a 3-mm i.d. copper tube, which is completely encased in stainless steel in order to avoid excessive contact potential differences with respect to its environment.

The atomic beam leaves the scattering cell through a large circular hole and is trapped immediately behind the cell by a liquid-nitrogen baffle. The baffle is provided with two bent pumping tubes to enable noncondensable gases to be pumped (e.g., helium gas used for energy calibra-

tion). The interior of the cell is lined with Mo micromesh to avoid electric field penetration from the outside through the large atomic beam outlet. The entrance and exit apertures for the atomic beam are also made of molybdenum. The entrance aperture was always 1 mm in diameter, whereas the exit aperture was varied between 1.5 and 14 mm. In order to provide more stable operation, the scattering cell is heated to 60 °C during the measurements.

The absolute measurements were carried out with the target cell shown in Fig. 3. In this case the mercury reservoir is water cooled rather than heated. All other parts are at room temperature or slightly heated. When the valve of the mercury supply is open, the scattering cell is connected to the reservoir and separated from the vacuum except for the small entrance aperture for the electron beam. When the valve is closed, the scattering cell is pumped through the valve body. Thus the target can also be switched on and off within a few seconds in this arrangement. The target pressure is measured by means of a capacitance manometer (MKSA Baratron 170 M; head type 310 BHS-1). The connection between the scattering cell and pressure gauge is heated and temperature controlled. The temperatures of the mercury reservoir and of the scattering cell are measured by calibrated Pt resistors. The diameters of entrance and exit apertures for the electrons are 1 and 4 mm, respectively; the length of the cell is $a = 40$ mm.

In each of the two target arrangements, both the scattering cell and the Faraday cup were insulated with high-quality insulators and normally connected to ground potential across the input resistors of two vibrating reed electrometers (Cary model 401). For test measurements, the Faraday cup was occasionally at potentials different from ground. In these cases both the exit of the scattering cell and the entrance of the screening of the Faraday cup were covered with Mo micromesh in order to avoid field penetration. Furthermore, an isolated electrometer (Keithley 616) was used instead of the vibrating reed.

PROCEDURE

An ideal electron beam for the present purposes should be infinitesimally narrow, parallel, and monochromatic, its energy should be well known, and the scattering cell should have infinitesimally small apertures.[7] If such an ideal beam with incident current I_0 travels a path length l within a homogeneous target having n atoms per unit volume, the unscattered exit current is, according to the well-known "absorption" or "attenuation" law

$$I = I_0 \exp(-nlQ), \tag{1}$$

where

$$Q = (nl)^{-1} \ln(I_0/I) \sim \ln(I_0/I) \tag{2}$$

is the total cross section. An absolute measurement of Q requires knowledge of n and l, whereas the relative shape of the cross-section curve versus energy E can be obtained even in an inhomogeneous target such as an atomic beam, if care is taken to keep the product of mean path length l and mean target density n constant during the measurement. In order to check the constancy of the factor $(nl)^{-1}$ during a relative run and in order to make runs with different values of $(nl)^{-1}$ comparable, it is advantageous to measure (absolute) ratios of cross sections

$$\frac{Q(E)}{Q(E_{\mathrm{ref}})} = \frac{\ln[I_0(E)/I(E)]}{\ln[I_0(E_{\mathrm{ref}})/I(E_{\mathrm{ref}})]}, \tag{3}$$

rather than relative cross sections themselves. E_{ref} is a suitably chosen reference energy (e.g., 6 eV in our low-energy data).

With target vapor, the electron currents I_s and I_c to scattering cell and Faraday cup ("collector") can be measured; the corresponding currents without target may be called I_{s0} and I_{c0} (Fig. 3). Thus, the values I_0 and I in Eqs. (2) and (3) could be identified in this case by "measurable" currents as follows:

$$I_0 = I_{s0} + I_{c0} = I_s + I_c; \quad I = I_c, \tag{4}$$

where I_{s0} should be zero in an ideal experiment.

Consequently, in an experimental arrangement without any energy analysis behind the target, an electron is considered as being "absorbed," if it is deflected by the target from its initial direction to such a degree that it no longer contributes to the current I_c. An energy loss without angular deflection could not be detected. This is not necessarily a disadvantage compared to the Ramsauer technique[7] having some energy analysis after scattering. At energies below the first inelastic threshold of mercury (4.67 eV), an energy analysis is not necessary because of the absence of inelastic processes. At higher energies, a high angular resoltuion can make up for a modest energy resolution, because inelastically scattered electrons also experience an angular deflection.[25-28] The minimum requirements for angular resolution have to be investigated, of course, otherwise the experimentally determined "effective" cross section could be smaller than the Q which is intended to be measured.

In our experiment, the currents reaching the scattering cell (I_s,I_{s0}) and those to the Faraday

cup (I_c,I_{c0}) were plotted on two xt recorders. The target was switched on and off repeatedly at a fixed energy, and the resulting curves bear resemblance to "square waves," which reveal any short time instability in intensity. In the case of relative measurements, slow drifts were eliminated by measuring cross-section ratios corresponding to Eq. (3). For reasons of stability, the current zero was determined by a large deflection of the electron beam within the lenses rather than by switching the cathode off.

The above analysis cannot be applied directly to a real experiment. Because of high demands on angular resolution, it is not desirable to make the exit aperture of the scattering cell large enough exactly to satisfy $I_{s0}=0$ in Eq. (4). It turned out in practice that keeping $I_{s0}<0.1I_{c0}$ is a reasonable compromise between demands on angular resolution and ease of interpretation of the measured data. The current balance Eq. (4) only holds if the incident current I_0 does not depend on whether the target is turned on or off. Using the scattering cell of Fig. 3, the current balance Eq. (4) could be verified within 1% measuring accuracy. In the target arrangement of Fig. 1, this balance could not be checked quantitatively because of the large exit hole for the atomic beam, through which an unknown portion of I_s disappears. Nevertheless, it seems to be a reasonable assumption that in this arrangement also, the incident current is not influenced by the target, because the cathode and the electron optical part are even better separated from the target region. Independently, an estimate based on the known pressure increase which occured in the lens system when turning on the atomic beam, and using the present cross sections, yields a loss of incident current of much less than 1% due to absorption in the lens system.

According to the practice[29] of necessarily non-ideal attenuation experiments,[7] the cross sections were evaluated by setting $I_0=I_{c0}$ and $I=I_c$ in Eqs. (2) and (3), although $I_{s0}<0.1I_{c0}\neq 0$ in our experiment. This procedure is somewhat doubtful,[7] but may be justified as follows: Electrons, which contribute to I_{s0} (i.e., those which do not pass through the exit aperture of the scattering cell without the target), have only a small chance of being deflected by the target exactly through the small exit hole. It is much more likely that even with the target present these electrons will hit the walls of the scattering cell somewhere else. If this is true, then I_{s0} must be completely neglected, because it never contributes to the process being observed. In order not to rely on this argument completely, I_{s0} has always been kept small compared to I_{c0}. In the case of the relative measurements, the possible error due to this simplified analysis is further reduced, because both of the current ratios in Eq. (3) are affected in the same way. It has also been checked experimentally whether the above assumption is justified. Within experimental accuracy, the relative cross sections obtained were not influenced by intentionally choosing $I_{s0}/I_{c0}=0.2$, 0.1, 0.05, and 0.03 at some representative energies; therefore the condition $I_{s0}/I_{c0}<0.1$ usually observed is sufficient. Similarly, the absolute cross sections remained unchanged when alternatively a somewhat more sophisticated evaluation method[30] was used.

The reliability of the measurements has been checked by further tests. One of the most important of these was the variation of target density, accomplished in each of the two target arrangements of Figs. 1 and 3 by variation of the temperature of the mercury reservoir. Using the atomic beam target, the temperature has been varied between 98 and 127 °C. This corresponds to vapor pressures inside the reservoir between 0.24 and 1.03 Torr,[31] the pressure within the atomic beam target being of course much lower. It turned out to be necessary to keep this temperature below 108 °C (or 0.4-Torr pressure), otherwise the measured cross-section ratios were not independent of the corresponding target densities. The reason is that at higher target densities the attenuation became extremely large. For example, at 127 °C the cross-section ratio $Q(0.4\text{ eV})/Q(6\text{ ev})$ was lowered by 30%, because there was a probability that one electron in 20 000 could reach the Faraday cup after a "forbidden" traverse of the atomic beam (favored by wall and multiple scattering). That means, at 0.4 eV and 127 °C a current ratio I_{c0}/I_c of 2×10^4 has actually been measured (point in Fig. 4), whereas one of about 10^6 would have been required to keep the cross-section ratio temperature independent (straight line in Fig. 4). Using the static target, the linear relation [Eq. (2)] between n and $\ln(I_{c0}/I_c)$ has been verified, which is a necessary condition for reliable attenuation experiments.[7]

With constant oven temperature, the size of the exit aperture of the scattering cell was varied in the arrangement of Fig. 1, in order to check the minimum requirements for angular resolution in the atomic beam arrangement. Within experimental errors, the shape of the relative cross section curve versus energy stayed constant, if the diameters at 0.1, 20, and 300 eV were not larger than 14, 5, and 3 mm, respectively. The smallest diameter used was 1.5 mm. When using the static target cell (Fig. 3), obtaining sufficient angular resolution is a very serious problem. Therefore this will be discussed in a separate sec-

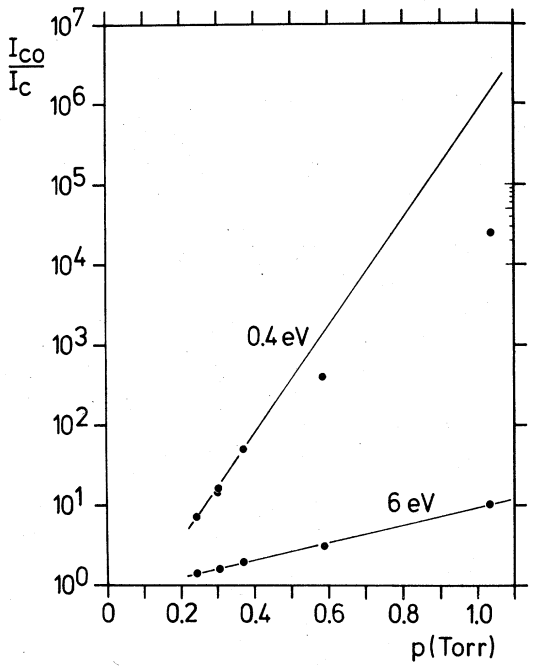

FIG. 4. Current ratio I_{c0}/I_c vs vapor pressure inside the mercury reservoir of the atomic beam oven. The pressure within the atomic beam itself is much lower. The straight line for 0.4 eV indicates the ratios I_{c0}/I_c which would be required to keep the cross-section ratio $Q(0.4\text{ eV})/Q(6\text{ eV})$ constant (see text).

tion in some detail.

By means of suitable positive potentials on the Faraday cup the possibly disturbing admixture of positive ions to the electron current has been investigated. The fraction of troublesome ions was negligible, if the target density was kept low enough. This was the case, if in the relative measurements, e.g., at 100 eV the attenuation $(I_{c0} - I_c)/I_{c0}$ was below 0.3. During the absolute measurements, this attenuation was chosen even lower than 0.2. The measurements below 10 eV are completely free of falsifying ions, because care has been taken to accelerate the electrons nowhere within the lens system to the first ionization threshold of mercury at 10.4 eV.

CORRECTION OF ABSOLUTE DATA FOR FINITE ANGULAR RESOLUTION

As emphasized above, poor angular resolution can be the most serious error source for determining total cross sections by attenuation experiments. The magnitude of this error depends mainly on the geometry of the scattering cell and on the angular distribution of the scattered electrons. In the case of single scattering (i.e., very low attenuation of the incident electron beam), the angular distribution of scattered electrons is directly given by the differential cross section $\sigma(\Theta,\Phi,E)$. Knowledge of σ at all scattering angles Θ between 0° and 180° yields the total cross section by integration:

$$Q(E)=\int_\Omega \sigma(\Theta,\Phi,E)\,d\Omega = 2\pi\int_0^\pi \sigma(\Theta,E)\sin\Theta\,d\Theta\,, \quad (5)$$

where the last expression is only valid if both electron beam and target are unpolarized and σ consequently is independent of the azimuth angle[2] Φ.

In an ideal attenuation experiment, integration of Eq. (5) is performed correctly by the apparatus itself, because none of the scattered electrons is allowed to pass through an infinitesimally small exit aperture in the scattering cell. If, however, the exit aperture has nonzero radius, a portion

$$A_0(\Theta_0)=\frac{2\pi\int_0^{\Theta_0}\sigma(\Theta,E)\sin\Theta\,d\Theta}{2\pi\int_0^{\pi}\sigma(\Theta,E)\sin\Theta\,d\Theta} \quad (6)$$

of the scattered electrons can pass through the exit aperture together with the unscattered electrons. Thereby Θ_0 is the half angle subtended by the exit hole as seen from the scattering center on the axis. Equation (6) has been integrated graphically using elastic differential cross sections[32] known from theory[20,33-35] or experiment.[1,36,37] The result for elastic scattering is shown in Fig. 5(a), whereas Fig. 5(b) shows equivalent curves for excitation to the $6\,^1P_1$ level based on experimental data[25,26] and extrapolation by means of the generalized oscillator strength described in these references. It should be noted

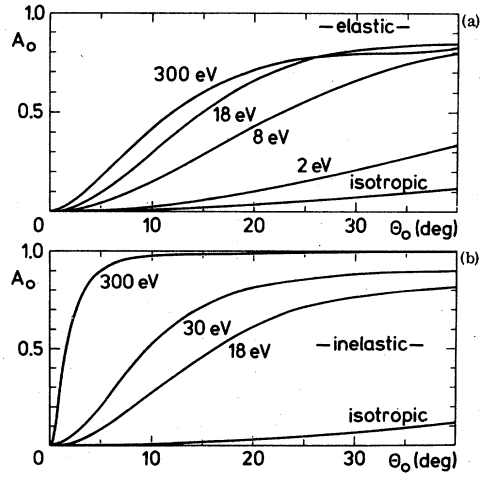

FIG. 5. Portion $A_0(\theta_0)$ of scattered electrons, which can pass through the exit aperture of the scattering cell. See Eqs. (6) and (7). A_0 for isotropic scattering is shown for comparison. (a) A_0 for elastic scattering, (b) A_0 for inelastic scattering (excitation to $6\,^1P_1$).

that the results of Fig. 5(b) probably only have low accuracy due to the extrapolation procedure. Fortunately, the absolute contribution of these less-reliable data to the total cross section is comparatively small and therefore less important.

The above considerations are valid for single scattering at an atomic beam target which is well concentrated at a distance x behind the entrance hole of the scattering cell. The static target used for the absolute measurements requires a further integration from $x = 0$ (entrance aperture) to $x = a$ (exit aperture). This is because the target cell is completely filled with target vapor. In order to perform this integration, A_0 in Eq. (6) has to be rewritten as a function of x rather than Θ_0. This can easily be accomplished by using the following relation [Fig. 6(a)]:

$$\Theta_0 = \tan^{-1}[r/(a-x)], \tag{7}$$

where r is the radius of the exit aperture.

Because the absolute measurements have been performed at rather low attenuation, i.e., $(I_{c0} - I_c)/I_{c0} < 0.2$, single scattering is predominant. Therefore, "scattering in" by a second scattering process of those electrons which were initially "scattered out" can be neglected. Neglecting also attenuation of the incident beam along its path through the target, i.e., assuming constant intensity along the axis of the scattering cell, yields by means of the above relations [Eqs. (6) and (7)]

$$B = \left(\int_0^a A(x)\,dx\right) \Big/ \left(\int_0^a dx\right), \tag{8}$$

where B is the fraction of scattered electrons, which is contained in the experimentally determined current I_c, although none of the scattered electrons should pass through the exit hole. If B were known, the ideally expected current I_c^i could be easily computed by subtracting the portion by which the measured I_c is too large:

$$I_c^i = I_c - B(I_{c0} - I_c^i), \tag{9a}$$

or

$$I_c^i = (I_c - BI_{c0})/(1 - B), \tag{9b}$$

where $I_{c0} - I_c^i$ in Eq. (9a) is the actual scattered-electron current.

The above results are valid, if only a narrow pencil beam of incident electrons travels along the axis of the target cell, and so angular spread of the primary beam is neglected. A real electron beam having angular spread can be considered to be a mixture of the case discussed above and of an annular portion of primary electrons passing near the periphery of the exit aperture. Due to the symmetry of the problem, this annular portion

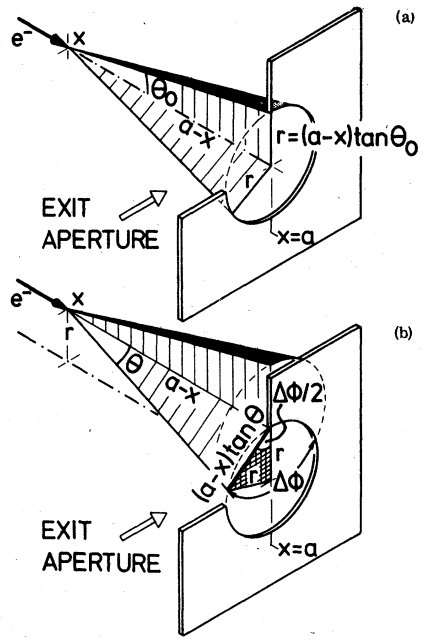

FIG. 6. (a) Geometry for derivation of Eq. (7). (b) Geometry for derivation of Eqs. (10a) and (10b). The cross-hatched triangle in the plane of the exit aperture having two sides of length r, one side of length $(a - x)\tan\theta$, and two equal angles of $\frac{1}{2}\Delta\phi$ is essential for obtaining Eq. (10b). Compare Fig. 3 for the actual geometry of the target cell.

can be represented by a single pencil beam aimed at the periphery, without loss of generality. By considering this representative beam parallel to the axis of the scattering cell, it can be shown, using simple trigonometric relations [Fig. 6(b)], that in this case

$$\Theta_{max} = \tan^{-1}[2r/(a-x)] \tag{10a}$$

and

$$\Delta\Phi = 2\cos^{-1}[(a-x)(\tan\Theta)/2r], \tag{10b}$$

i.e., only those electrons which are scattered by less than Θ_{max} have a chance of passing through the exit aperture, and of these only a Θ dependent portion $\Delta\Phi$ of the full azimuth will actually be accepted.

Equations (10a) and (10b) are also approximately valid, if the incident beam is slightly inclined with respect to the axis but still passes very close to the rim of the exit aperture. The corresponding expression to Eq. (6) for such a beam is now

$$A_r(\Theta) = \frac{\int_0^{\Theta_{max}} \Delta\Phi(\Theta)\sigma(\Theta, E)\sin\Theta\,d\Theta}{2\pi\int_0^{\pi}\sigma(\Theta, E)\sin\Theta\,d\Theta}, \tag{11}$$

which can be used alternately in Eq. (8) in order to evaluate the ideally expected current I_c^i in Eq. (9b) for a divergent primary beam.

Employing the results of Fig. 5(a) at 18 eV (which are similar to those of Fig. 5(b) at this energy), Eq. (8) has been solved by graphic integration both for $A_0(x)$ [Eqs. (6) and (7)] and for $A_r(x)$ [Eqs. (10) and (11)]. A value of 18 eV has been used as a representative energy for the energy range covered by the absolute measurements. Using the geometry of our target cell ($a = 40$ mm, $r = 2$ mm), we obtained $B_{max} = 0.25$ and $B_{min} = 0.14$ by introducing either A_0 or A_r in Eq. (8). We decided to take an average value of $B = 0.2$, which is slightly closer to the upper limit. The reason is that the electron beam was always carefully centered, thus the true value should be closer to the upper limit, which is valid for an axial pencil beam. Furthermore, neglecting electrons which possibly are "scattered in" from I_{s0} would result in a larger value of B. On the other hand, neglecting attenuation of the incident beam and neglecting backscattering of electrons from the Faraday cup into the scattering cell (either by target vapor or walls) results in a slight overestimation of B in Eq. (8). The average value chosen seems to be a fair compromise. Taking up again the arguments of the preceding section, I_{s0} has been neglected completely, and the total cross sections at the absolute measurements have been evaluated by identifying I_{c0} and I_c^i [Eq. 9(b)] with I_0 and I in Eq. (2), i.e.,

$$Q = (na)^{-1} \ln[I_{c0}(1-B)/(I_c - BI_{c0})]$$
$$= (na)^{-1} \ln[0.8I_{c0}/(I_c - 0.2I_{c0})]. \quad (12)$$

Introducing this correction has a rather big influence on the computed cross section. In our case, the total cross sections around 20 eV are about 30% larger than the uncorrected ones [Eq. (2)], see Fig. 7. At very low energies the demands on angular resolution—and seemingly the influence of the correction—were less stringent. However, at low energies larger exit apertures had to be used in order to keep the ratio I_{s0}/I_{c0} small. Furthermore, in order to apply the above correction, very low attenuation had to be used so that the resonances for energy calibration were hardly visible. Without a safe guide for energy calibration, we preferred a less critical energy region for the absolute measurements.

ENERGY CALIBRATION

As mentioned above, at low energies (<15 eV) an accurate energy calibration is necessary because of unknown contact potentials and thermal energy. The calibration was performed in the arrangement of Fig. 1 using the distinct resonances of mercury at 4.91 and 5.50 eV by recording either I_c or I_s versus the voltage between cathode tip and scattering cell. An example of such a plot is shown in Fig. 8. This procedure was repeated about every 20 min during a low-energy run in order to perceive any possible drift of contact potential. The calibration (including temporal stability) was accurate to better than ±30 meV.

When the experiment was planned and started, the energy position of these mercury resonances was not known reliably. Therefore, their position has been determined by means of the well-known

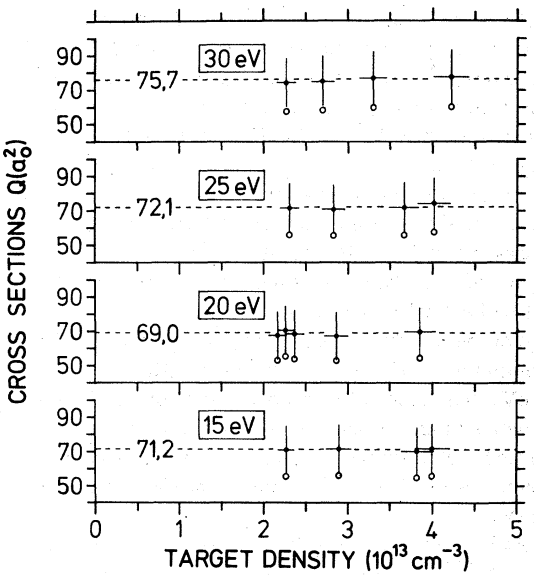

FIG. 7. Results of absolute cross-section measurements vs target density. Open circles, uncorrected results corresponding to Eq. (2). Black dots with error bars, results corrected for finite angular resolution corresponding to Eq. (12). The dashed lines show the mean value of the corrected results.

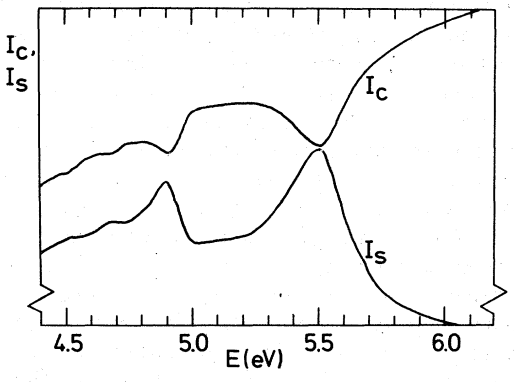

FIG. 8. Recorder plots of I_c and I_s vs energy showing the resonances at 4.91 and 5.50 eV which were used for energy calibration. In this case the accelerating voltage was about 1.5 V lower than the corresponding electron energy shown in the figure (i.e., the contact potential was about 1.5 eV). Zero greatly suppressed.

helium resonance at 19.37 eV, of which the position is known at least to within ±10 meV.[38] For this purpose, a mixture of He and Hg was used in the atomic beam arrangement, in order to plot the resonances of He and Hg simultaneously. The mixing ratio was varied up to the limits of visibility of each of the resonances in order to detect a possible pressure dependence of their positions; such a dependence could not be observed. The positions of the two resonances utilized were determined to be 4.91 ± 0.02 eV and 5.50 ± 0.02 eV in good agreement with recent results.[13,14,17] The helium resonance, whose natural halfwidth is below 10 meV, has also been used to determine the energy spread of the electron beam leaving the monochromator. The energy profile turned out to be approximately triangular with a halfwidth of 100 meV.

At higher energies (>15 eV) the energy dependence of the cross sections is small. Therefore, the requirements for energy calibration and energy halfwidth are less stringent. In the arrangement of Fig. 2 without monochromator, the halfwidth was about 500 meV. The calibration in this case was made by means of a retarding potential method[29] and was accurate within ±300 meV; at higher energies the calibration was accurate within ±0.1%.

EXPERIMENTAL ERRORS

In principle, the cross sections were determined by means of Eqs. (2) and (3). Therefore, errors may be introduced by any of the quantities to be found there, often in a rather involved manner as partly discussed above.

The current measurement itself was no problem, of course, because even in the case of absolute measurements only current ratios are required, i.e., one has only to rely on the linearity of the electrometers used and not on their absolute calibration. The linearity of the three instruments used could easily be cross checked. Also noise was no problem (except for the highest attenuations used for tests), because the incident current $I_0 \approx I_{c0}$ was kept in the range 10^{-9}–10^{-10} A. The most serious indirect effects on the current measurement (poor angular resolution, ions, influence of target vapor on the cathode) have been discussed above and could be either avoided or approximately corrected for. A further estimate showed also that backscattering of electrons from the Faraday cup to the target cell (either by target vapor or by its walls[39,40]) has a negligible effect.

The accuracy of the pressure gauge used for absolute measurements was checked by means of an accurate U-tube oil manometer between 0.1 and 1 Torr and was found to agree there with the factory calibration within ±1% when no correction for thermal transpiration[41] ("Knudsen effect") was applied. Consequently, this correction was omitted. In our case the theoretical correction would be below 3% anyway, which is small compared to other uncertainties in the absolute measurements and probably overestimates the actually observable effect considerably.[37] Independently, the pressure in the target cell was determined by means of known vapor pressures[31] and roughly known conductivities of the connections between mercury reservoir, target cell, and vacuum system. This rather unreliable estimate agreed with the pressure reading within 20%.

Thus summarizing the above considerations and taking into account the reproduciblity of the data, the energy is known to within ±30 meV (at higher energies within ±0.1%). The energy spread, by which the $Q(E)$ curves could be affected, amounts to 100 meV FWHM (at higher energies 500 meV). The error of the relative cross-section curve is estimated to be ±3% between 0.3 and 100 eV. At lower and at higher energies the error increases gradually to about twice this value, due to increasing experimental difficulties such as handling low-energy beams and obtaining sufficient angular resolution especially for inelastic scattering [Fig. 5(b)]. The relative error of immediately neighboring data points (e.g., within a resonance) is below 1%.

The absolute data have two additional uncertainties each of about ±10%. One of these is the uncertainty in the factor B in Eq. (12), which corrects for limited angular resolution. The other one is due to uncertainties of the factor $(nl)^{-1}$ in Eq. (2), both because of errors in n (pressure determination) but mainly because of target vapor escaping through the entrance aperture of the scattering cell into the vacuum system. Therefore, the incoming electrons do not experience an immediate pressure rise at the entrance hole, i.e., the length a of the scattering cell [Eq. (12)] is not necessarily identical with the effective path length l of the electrons within the target. The total error of our absolute data is estimated to be about ±15%. This error appears to be rather high compared to other modern experiments in this field. In light of the above discussion, however, we do not think that this estimate is too conservative.

RESULTS AND COMPARISON WITH OTHER DATA

The present results are shown in Figs. 9–11 and in Table I. Direct measurements of other authors are compared with the present data in Fig. 9. Most of these results were obtained more than 40

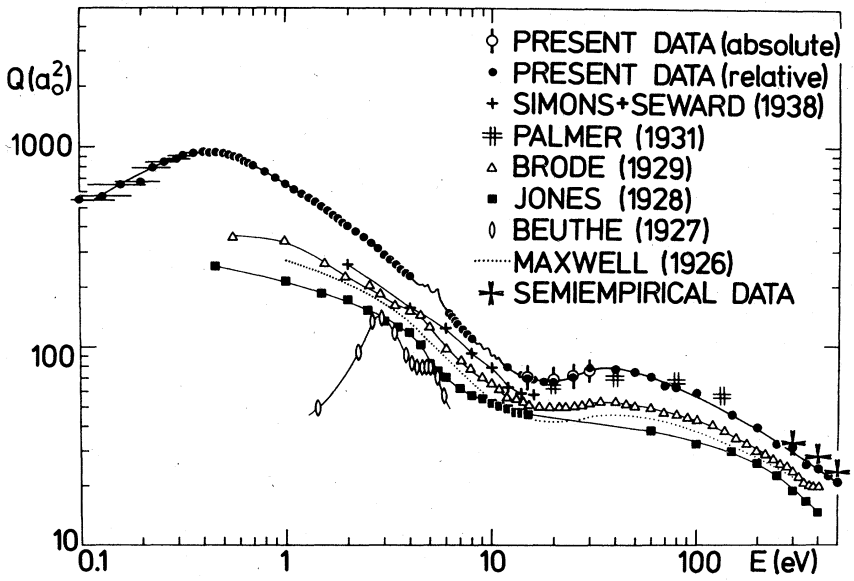

FIG. 9. Comparison of the present results with cross-section measurements of other authors. Our relative data are normalized to our corrected absolute data shown in Fig. 7.

years ago, except for the semiempirical data at 300, 400, and 500 eV, where more recent data were partly employed. These semiemprical total cross sections are obtained by summing elastic, excitation, and ionization cross sections. Thereby the total elastic cross section was computed by means of Eq. (5) using experimental absolute values[37] of σ for scattering angles $\Theta \leq 20°$, supplemented by theoretical values[33-35] for $\Theta \geq 20°$.

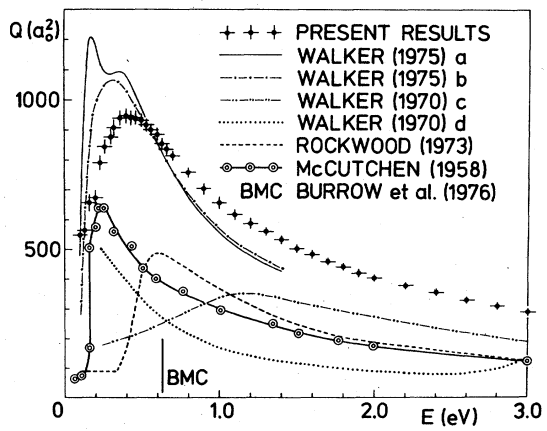

FIG. 10. Comparison of the present data with theoretical calculations and with experimental momentum transfer cross sections. The vertical line marked BMC shows the energetic position of the cross-section maximum found by Burrow *et al.* (Ref. 15). All calculations of Walker (Refs. 20 and 21) shown in this plot are relativistic. They are distinguished as follows: (a) including polarization and exchange with all target electrons; (b) including polarization and exchange with outermost three shells of target; (c) including exchange, without polarization; (d) without exchange and polarization.

Although the theoretical values are absolute, they were considered to be relative for this purpose and fitted at $\Theta = 20°$ to the absolute experiment.[37] The relative shape of the theoretical σ has in fact been verified experimentally elsewhere.[36] In a similar way, the total excitation cross section was estimated using experimental differential cross sections for excitation to the $^1P_1$ level[26]; excitation to other levels should contribute less than a total of 10% to the excitation in this energy range and were therefore neglected. Finally, the "gross ionization cross section"[42] measured by Smith[43] was reduced to the "counting cross section" needed here by means of other data.[44] For the total elastic cross section at 300, 400, and 500 eV we obtained the values $17.0a_0^2$, $13.8a_0^2$, and $11.9a_0^2$. For

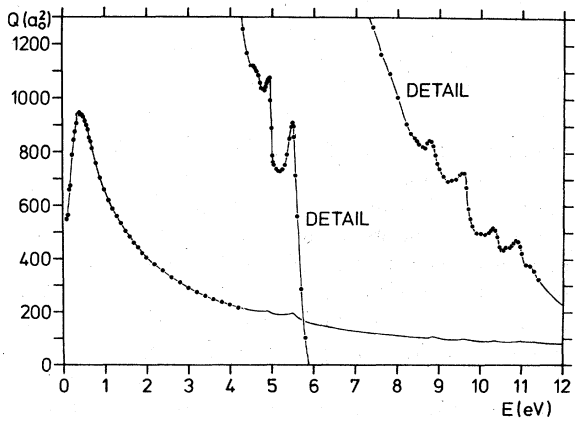

FIG. 11. Resonance structure of present results. Ordinate of details 25 ×enlarged; zero suppressed by $160a_0^2$ and $70a_0^2$, respectively.

TABLE I. Total cross sections for electron-mercury scattering. Absolute accuracy about ± 15%. Relative errors of immediately neighboring data points below 1%.

E (eV)	$Q(a_0^2)$	E (eV)	$Q(a_0^2)$	E (eV)	$Q(a_0^2)$	E (eV)	$Q(a_0^2)$
0.10	548.0	4.00	227.1	6.40	142.5	10.30	90.7
0.13	563.8	4.20	216.1	6.60	136.7	10.35	90.4
0.16	657.7	4.30	210.2	6.70	133.4	10.40	89.4
0.20	673.3	4.40	206.7	6.80	131.1	10.45	87.9
0.23	790.8	4.50	204.8	6.90	129.0	10.50	87.4
0.26	845.6	4.54	204.8	7.00	127.2	10.55	87.4
0.30	877.0	4.58	204.5	7.20	123.6	10.60	87.9
0.32	908.3	4.62	204.0	7.40	120.6	10.70	87.9
0.36	939.6	4.66	203.4	7.60	116.5	10.75	88.2
0.40	947.4	4.70	202.3	7.80	113.7	10.80	88.5
0.43	939.6	4.74	201.5	8.00	110.3	10.85	88.8
0.46	939.6	4.78	201.4	8.20	106.3	10.90	88.6
0.50	931.8	4.82	201.2	8.30	104.9	10.95	88.0
0.53	916.1	4.84	201.7	8.40	104.2	11.0	86.9
0.56	900.5	4.86	202.3	8.45	103.8	11.1	85.2
0.60	884.8	4.88	203.6	8.50	103.4	11.2	85.0
0.63	853.5	4.90	203.8	8.60	102.9	11.3	84.3
0.66	837.8	4.92	203.0	8.65	102.7	11.4	83.0
0.70	814.3	4.94	199.7	8.70	103.5	12.0	79.1
0.80	759.5	4.96	195.4	8.75	103.8	14.0	72.8
0.90	704.7	5.00	191.5	8.80	103.7	15.0	69.7
1.00	657.7	5.02	190.4	8.85	103.0	16.0	68.3
1.10	618.6	5.04	190.1	8.90	101.6	18.0	67.2
1.20	587.3	5.10	189.5	8.95	100.4	20.0	67.3
1.30	560.6	5.15	189.2	9.00	99.6	25.0	70.3
1.40	534.0	5.20	189.2	9.10	98.5	30.0	78.3
1.50	502.7	5.25	189.5	9.20	97.7	40.0	76.7
1.60	483.9	5.30	190.1	9.30	97.9	50.0	75.2
1.70	460.4	5.35	191.7	9.40	98.0	60.0	70.6
1.80	443.2	5.40	194.0	9.50	98.8	70.0	63.9
1.90	421.3	5.45	195.8	9.55	99.0	80.0	62.6
2.00	404.0	5.47	196.4	9.60	99.0	100.0	59.0
2.20	380.5	5.50	195.9	9.65	96.8	150.0	45.7
2.40	357.0	5.52	194.3	9.70	93.6	200.0	39.6
2.60	330.8	5.55	188.5	9.75	92.1	250.0	32.6
2.80	311.6	5.60	182.4	9.80	91.0	300.0	31.3
3.00	289.7	5.70	171.5	9.90	89.9	350.0	25.4
3.20	274.1	5.80	164.1	10.00	89.9	400.0	24.1
3.30	260.0	5.90	159.1	10.10	89.7	450.0	22.4
3.60	247.4	6.00	156.6	10.20	90.1	500.0	20.7
3.80	237.2	6.20	148.9	10.25	90.4		

the same sequence of energies the excitation cross sections $4.7a_0^2$, $3.8a_0^2$, and $3.2a_0^2$ and the counting ionization cross sections $11.2a_0^2$, $9.5a_0^2$, and $8.3a_0^2$ were obtained. The resulting total cross sections are $Q(300\text{ eV}) = 32.9a_0^2$, $Q(400\text{ eV}) = 27.1a_0^2$, and $Q(500\text{ eV}) = 23.4a_0^2$, each with an estimated uncertainty of ±10%. The agreement with our directly measured data is well within the combined errors.

An obvious trend of the direct measurements can be seen in Fig. 9: In general, the more-recent data come closer to the present data. Nevertheless, with one exception,[45] all other direct experiments describe the general shape of the total cross section versus energy reasonably well. Most of these experiments employed either the Brode modification of Ramsauer's technique[3,4] or a simple linear arrangement without monochromator.[4-6,46] Jones[4] used both techniques. His results gained by the linear technique are not shown in Fig. 9, because they almost duplicate Brode's results.[3] Jones' results gained by the Brode technique are much lower and are shown in the figure. Looking, however, at his drawing of the apparatus, one gets the impression that the first 45° of the circular beam path belong to the electron gun ra-

ther than to the scattering region, because there is a narrow limiting slit at the 45° position which collimates the probably diffuse primary beam. If this were true, the path length would be shorter than he assumed, and consequently [Eq. (2)] his cross sections would be about 25% larger, in good agreement with his own results using the linear technique and with Brode's results. Only one experiment used the original Ramsauer technique[45] which yielded in this case the least-reliable results, although this technique is considered superior to the Brode technique.[7,30] The somewhat strange results of Beuthe's work have most likely to be attributed to vacuum problems, to temporal instabilities, and to his extremely short Faraday collector.

In general, the cross sections measured around 1930 are much lower than the present results, in contrast to the measurements on alkali vapor targets, where old measurements yield much larger cross sections than recent ones.[7] Almost surprisingly good agreement (within 10%) is found, however, with the data of Palmer,[5] who made an experimental analysis of angular resolution at a few energies. Extrapolating his "absorption coefficient" to the limiting angle zero, one obtains cross sections of $63a_0^2$, $70a_0^2$, $67a_0^2$, and $57a_0^2$ at 20, 40, 80, and 135 eV. This agreement supports our assumption that most of the older measurements are too low due to lack of sufficient angular resolution. The deviations may also be partly due to errors in determining the target density via vapor pressure tables. This was already recognized by Brode,[3] who used vapor-pressure data,[47] which are almost 10% higher than recent ones.[31] Taking this into account, his cross sections are about 10% larger than shown in Fig. 9 in better agreement with the present results. Further criticism can be found in the literature.[7]

In Fig. 10 our total cross sections are compared with momentum transfer cross sections[8,9] Q_{MT}. The agreement is very poor. This is not too astonishing because of the different definition[48] of Q measured here and Q_{MT}.[7,10,49] These two cross sections could only agree if either the differential cross section σ were isotropic [$\sigma(\Theta) = \text{const}$] or, more generally, if $\sigma(\Theta) = \sigma(\pi - \Theta)$. It has been shown experimentally[50] and theoretically[33] that neither is the case in e^--Hg scattering, even at low energies around 1 eV. Using theoretical values of $\sigma(\Theta)$, one obtains, e.g., at 2 eV a ratio Q/Q_{MT} of almost 2 due to their different definition; this ratio is energy dependent. The disagreement between the Q_{MT} experiments themselves is probably due to the very involved analysis of transport data. Nevertheless, the existence of a cross-section maximum below 1 eV is verified independently by these experiments. It is interesting to note that a phase-shift analysis by Hutt[19] is consistent with a cross-section maximum at about 0.6 eV as suggested by the more recent Q_{MT} values.[9] However, according to this analysis, it is also consistent with a higher maximum at lower energies, as occurs in the present results.

Several recent e^--Hg scattering experiments were performed to determine the energetic position of resonances rather than total cross sections (see, e.g., Refs. 12–17 and papers quoted there). One of the most recent of these[15] was the first to find a cross-section maximum below 1 eV by means of a transmission technique. The energetic position of this maximum, which is probably a $(6s^26p_{1/2})^2P_{1/2}$ shape resonance,[15,21] was determined to be 0.63 ± 0.03 eV in excellent agreement with the maximum in Q_{MT} found by Rockwood.[9] Nevertheless, these two results are in contradiction to the present results, where the maximum occurs at 0.4 eV (Fig. 10), and we think that their mutual agreement is fortuitous. The agreement of these quoted results may partly be due to favoring large scattering angles in both experiments. For momentum transfer experiments, this follows immediately from definition.[48] In the transmission experiment[15] a trochoidal monochromator[51] has been used. This type of monochromator has proved to be a very successful and accurate instrument for locating *sharp* structures.[52] It is very difficult, however, to analyze the angular resolution obtained in the scattering cell, which is also exposed to a comparatively high longitudinal magnetic field. When *broad* features are to be located energetically, any energy dependence of angular resolution and of primary intensity should be known accurately, otherwise the location could become erroneous. Following an analysis of Simpson,[53] the combination of a magnetic field (~150 G) together with a retarding potential (electron energy reduced to less than 200 meV) should deteriorate the angular resolution with decreasing primary energy. According to our (probably too crude and oversimplified) estimate, this deterioration should be particularly drastic below 1 eV, and not strongly dependent on the retarding voltage applied. If this rough estimate holds true at least qualitatively, the cross section maximum below 1 eV would appear at an energy which is somewhat too high, and its erroneous position would not be changed essentially by variation of the retarding potential within a factor 2. This analysis could possibly explain the excellent agreement between their and our location[14,15] of sharp resonances above 4 eV and the less satisfying agreement of the energetic position of the broad maximum below 1 eV.

This explanation is supported by the shift of the maximum in question to lower energies, when the target pressure was raised in the experiment employing the trochoidal monochromator. It seems probable that multiple scattering is responsible for this effect. It is possible, however, that multiple scattering facilitates obtaining sufficient angular resolution, because several small and hence undetectable deflections of singly scattered electrons may lead to an observable deflection. This means that a forward peaked angular distribution of singly scattered electrons appears macroscopically to be more isotropic when multiple scattering occurs and so can compensate for an angular resolution which is too small. In our experiment, the energetic position of this maximum was independent of target pressure in the range investigated.

In Fig. 10, the present results are also compared with theoretical cross sections. There exists a variety of calculations at higher energies,[33-35] which concentrate on spin polarization[2] and differential cross sections for elastically scattered electrons. From these data one could obtain total elastic cross sections either by solving Eq. (5) or, more conveniently, by employing the optical theorem. Nevertheless, elastic data are comparable directly with our results only below the first inelastic threshold, where theoretical data are scarce. To our knowledge, the only suitable data for e^--Hg scattering at low energies are those of Walker,[20,21] who made relativistic calculations with and without exchange as well as charge-cloud polarization. Both his latest results[21] (relativistic, including polarization and two different degrees of exchange) are in qualitative agreement with our data, although his resonant cross-section maximum (in one case split) occurs at lower energies. In order to ensure that this energy shift is not caused by our nonideal energy resolution, we folded the theoretical curves with a triangular-shaped energy distribution of 200-meV basewidth, which corresponds to the energy spread of our electron beam. The influence of this procedure on the energetic position of the theoretical cross-section maxima is almost negligible. Therefore, the nonideal energy resolution of the experiment is not responsible for the differences. It is more likely that the calculation is very sensitive to the approximation used. This is suggested by the comparatively large effect caused by a slight change of the degree of exchange used. Also the polarization, which is computed by means of the polarized orbital method, has a large effect. Walker thinks that the distortion of the atom by the incident electron is probably overestimated in his approximation; taking less polarization into account would shift the peak to higher energies in better agreement with the experiment. Neglecting polarization altogether yields a cross-section curve[20] without much resemblance to the experimental one (Fig. 10). Neglecting exchange as well even yields monotonically decreasing cross sections with increasing energy.[20] This indicates that low-energy-electron scattering in mercury is largely governed by exchange and polarization (distortion) effects.

ACKNOWLEDGMENTS

We wish to express our thanks to Professor J. Kessler for his advice and encouragement, and to the staff of the machine shop who willingly executed the numerous alterations up to the final version of the apparatus. We also gratefully acknowledge the help of Dr. C. B. Lucas in improving the readability of the manuscript. Furthermore, we appreciate the generous support of the Deutsche Forschungsgemeinschaft for this work.

[1] L. J. Kieffer, At. Data 2, 347 (1971).
[2] J. Kessler, Rev. Mod. Phys. 41, 3 (1969); *Polarized Electrons* (Springer-Verlag, Berlin, 1976).
[3] R. B. Brode, Proc. R. Soc. London Ser. A 125, 134 (1929).
[4] T. J. Jones, Phys. Rev. 32, 459 (1928).
[5] R. R. Palmer, Phys. Rev. 37, 70 (1931).
[6] J. H. Simons and R. P. Seward, J. Chem. Phys. 6, 790 (1938).
[7] B. Bederson and L. J. Kieffer, Rev. Mod. Phys. 43, 601 (1971).
[8] C. W. McCutchen, Phys. Rev. 112, 1848 (1958).
[9] S. D. Rockwood, Phys. Rev. A 8, 2348 (1973).
[10] Y. Itikawa, At. Data Nucl. Data Tables 14, 1 (1974).
[11] H. S. W. Massey, E. H. S. Burhop, and H. B. Gilbody, *Electronic and Ionic Impact Phenomena* (Clarendon, Oxford, 1969), Vol. I (a) p. 47, (b) p. 29.
[12] C. E. Kuyatt, J. A. Simpson, and S. R. Mielczarek, Phys. Rev. 138, A385 (1965).
[13] T. W. Ottley and H. Kleinpoppen, J. Phys. B 8, 621 (1975).
[14] P. D. Burrow and J. A. Michejda, International Symposium on Electron and Photon Interactions with Atoms, Stirling 1974, Abstracts of contributed papers, p. 50.
[15] P. D. Burrow, J. A. Michejda, and J. Comer, J. Phys. B 9, 3225 (1976).
[16] D. W. O. Heddle, J. Phys. B 8, L33 (1975), and papers quoted there.
[17] K. Albert, C. Christian, T. Heindorff, E. Reichert and S. Schön, J. Phys. B 10, 3733 (1977).
[18] P. K. Hutt and B. H. Bransden, J. Phys. B 7, 2223 (1974).
[19] P. K. Hutt, J. Phys. B 8, L88 (1975).

[20]D. W. Walker, Adv. Phys. 20, 257 (1971); J. Phys. B 3, L123 (1970).
[21]D. W. Walker, J. Phys. B 8, L161 (1975) and private communications.
[22]W. Schmitz and W. Mehlhorn, J. Phys. E 5, 64 (1972), and papers quoted therein.
[23]D. W. O. Heddle, J. Phys. E 4, 981 (1971); JILA Rep. No. 104, University of Colorado, 1970.
[24]A. Adams and F. H. Read, J. Phys. E 5, 156 (1972).
[25]F. Hanne and J. Kessler, Phys. Rev. A 5, 2457 (1972).
[26]A. Skerbele and E. N. Lassettre, J. Chem. Phys. 52, 2708 (1970); 56, 845 (1972).
[27]K.-H. Gronemeier, Z. Phys. 232, 483 (1970).
[28]J. N. Bass, R. A. Berg, and A. E. S. Green, J. Phys. B 7, 1853 (1974).
[29]C. E. Kuyatt, in *Methods of Experimental Physics*, Vol. 7A, edited by B. Bederson and W. L. Fite (Academic, New York and London, 1968), p. 1.
[30]D. E. Golden and H. W. Bandel, Phys. Rev. 138, A14 (1965).
[31]Landolt-Börnstein, *Zahlenwerte und Funktionen* (Springer-Verlag, Berlin, 1960), Vol. II, 2a, p. 19.
[32]Even relative σ values can be used, because the denominator of Eq. (6) has not to be identified necessarily with the absolute Q of Eq. (5). When using theoretical data, however, only those which take charge-cloud polarization into account yield reliable values; neglecting distortion in theory underestimates the important contribution of small scattering angles [see, e.g., D. Herrmann, K. Jost, J. Kessler, and M. Fink, J. Chem. Phys. 64, 1 (1976)].
[33]D. W. Walker, J. Phys. B 3, 788 (1970), and private communication.
[34]G. Holzwarth and H. J. Meister, Nucl. Phys. 59, 56 (1964), and unpublished.
[35]M. Fink and A. C. Yates, At. Data 1, 385 (1970).
[36]J. Kessler and H. Lindner, Z. Phys. 183, 1 (1965).
[37]J. P. Bromberg, J. Chem. Phys. 51, 4117 (1969).
[38]S. Cvejanović, J. Comer, and F. H. Read, J. Phys. B 7, 468 (1974).
[39]P. Marmet and L. Kerwin, Can. J. Phys. 38, 787 (1960).
[40]E. H. Darlington and V. E. Cosslett, J. Phys. D 5, 1969 (1972).
[41]See, e.g., S. Dushman, *Scientific Foundations of Vacuum Technique* (Wiley, New York, 1949), pp. 65 and 90, or other textbooks on vacuum technique.
[42]See, e.g., L. J. Kieffer and G. H. Dunn, Rev. Mod. Phys. 38, 1 (1966).
[43]P. T. Smith, Phys. Rev. 37, 808 (1931).
[44]W. Bleakney, Phys. Rev. 35, 139 (1930).
[45]H. Beuthe, Ann. Phys. (Leipz.) 84, 949 (1927).
[46]L. R. Maxwell, Proc. Natl. Acad. Sci. 12, 509 (1926).
[47]Landolt-Börnstein, *Physikalisch-Chemische Tabellen* (Springer-Verlag, Berlin, 1923), Vol. II, p. 1335.
[48]Q is defined by Eq. (5). Q_{MT} is defined by replacing σ by $\sigma(1-\cos\theta)$ in this equation [see Refs. 7, 10, 11(a), 49].
[49]L. S. Frost and A. V. Phelps, Phys. Rev. 136, A1538 (1964).
[50]M. Düweke, N. Kirchner, E. Reichert, and S. Schön, J. Phys. B 9, 1915 (1976), and papers quoted therein.
[51]A. Stamatovic and G. J. Schulz, Rev. Sci. Instrum. 41, 423 (1970).
[52]G. J. Schulz, Rev. Mod. Phys. 45, 378 (1973).
[53]J. A. Simpson, Rev. Sci. Instrum. 32, 1283 (1961).